Oxidovanadium(IV/V) Complexes as New Redox Mediators in Dye-Sensitized Solar Cells: A Combined Experimental and Theoretical Study

ARTICLE *in* INORGANIC CHEMISTRY · APRIL 2015

Impact Factor: 4.76 · DOI: 10.1021/acs.inorgchem.5b00159 · Source: PubMed

9 AUTHORS, INCLUDING:

Manos Vlasiou
University of Cyprus
6 PUBLICATIONS **12** CITATIONS
SEE PROFILE

Elias Stathatos
Technological Educational Institute of West…
107 PUBLICATIONS **2,981** CITATIONS
SEE PROFILE

Inorganic Chemistry

Article

pubs.acs.org/IC

Oxidovanadium(IV/V) Complexes as New Redox Mediators in Dye-Sensitized Solar Cells: A Combined Experimental and Theoretical Study

Andigoni Apostolopoulou,[†,∥] Manolis Vlasiou,[‡] Petros A. Tziouris,[§] Constantinos Tsiafoulis,[#] Athanassios C. Tsipis,*[,§] Dieter Rehder,*[,⊥] Themistoklis A. Kabanos,*[,§] Anastasios D. Keramidas,*[,‡] and Elias Stathatos*[,†]

[†]Nanotechnology and Advanced Materials Laboratory, Electrical Engineering Department, Technological-Educational Institute of Western Greece, GR-26334 Patras, Greece

[‡]Department of Chemistry, University of Cyprus, Nicosia 1678, Cyprus

[§]Section of Inorganic and Analytical Chemistry, Department of Chemistry and [#]NMR Center, University of Ioannina, Ioannina 45110, Greece

[⊥]Department of Chemistry, University of Hamburg, D-20146 Hamburg, Germany

[∥]Department of Physics, University of Patras, GR-26500 Patras, Greece

Supporting Information

ABSTRACT: Corrosiveness is one of the main drawbacks of using the iodide/triiodide redox couple in dye-sensitized solar cells (DSSCs). Alternative redox couples including transition metal complexes have been investigated where surprisingly high efficiencies for the conversion of solar to electrical energy have been achieved. In this paper, we examined the development of a DSSC using an electrolyte based on square pyramidal oxidovanadium(IV/V) complexes. The oxidovanadium(IV) complex $(Ph_4P)_2[V^{IV}O(hybeb)]$ was combined with its oxidized analogue (Ph_4P)-$[V^{V}O(hybeb)]$ {where $hybeb^{4-}$ is the tetradentate diamidodiphenolate ligand [1-(2-hydroxybenzamido)-2-(2-pyridinecarboxamido)benzenato}and applied as a redox couple in the electrolyte of DSSCs. The complexes exhibit large electron exchange and transfer rates, which are evident from electron paramagnetic resonance spectroscopy and electrochemistry, rendering the oxidovanadium(IV/V) compounds suitable for redox mediators in DSSCs. The very large self-exchange rate constant offered an insight into the mechanism of the exchange reaction most likely mediated through an outer-sphere exchange mechanism. The $[V^{IV}O(hybeb)]^{2-}/[V^{V}O(hybeb)]^{-}$ redox potential and the energy of highest occupied molecular orbital (HOMO) of the sensitizing dye N719 and the HOMO of $[V^{IV}O(hybeb)]^{2-}$ were calculated by means of density functional theory electronic structure calculation methods. The complexes were applied as a new redox mediator in DSSCs, while the cell performance was studied in terms of the concentration of the reduced and oxidized form of the complexes. These studies were performed with the commercial Ru-based sensitizer N719 absorbed on a TiO_2 semiconducting film in the DSSC. Maximum energy conversion efficiencies of 2% at simulated solar light (AM 1.5; 1000 W m^{-2}) with an open circuit voltage of 660 mV, a short-circuit current of 5.2 mA cm^{-2}, and a fill factor of 0.58 were recorded without the presence of any additives in the electrolyte.

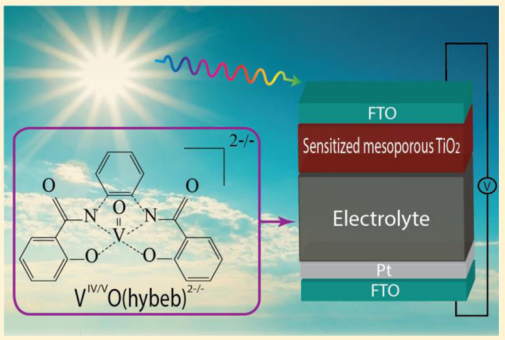

INTRODUCTION

Vanadium compounds are of great interest due to their biological importance,[1−3] catalytic activity,[4−8] and their use in alternative electrochemical energy storage technologies (i.e., batteries).[9] Moreover, oxidovanadium(IV/V) compounds, such as $[VO(salen)]^{0/+}$,[10] which exhibit reversible redox behavior, might be essential in various electrochemical devices, such as redox mediators in dye-sensitized solar cells (DSSCs).[11]

Third-generation DSSCs have been recognized as a low-cost viable alternative to conventional amorphous silicon photovoltaics.[12,13] The unique design of DSSCs offers choices for changing the materials of the different parts that constitute DSSCs to improve their performance. The components of a typical DSSC have more or less been standardized, and they are a TiO_2 nanocrystalline film deposited on fluorine-doped tin dioxide (SnO_2:F) transparent conductive electrode (negative electrode), a ruthenium bipyridyl derivative adsorbed and chemically anchored on TiO_2 nanocrystallites, an electrolyte bearing I^-/I_3^- redox mediator, and a platinized SnO_2:F electrode (positive electrode). A fundamental component of the DSSC is the redox couple in the electrolyte. The I^-/I_3^- redox couple is

Received: January 22, 2015

DOI: 10.1021/acs.inorgchem.5b00159
Inorg. Chem. XXXX, XXX, XXX−XXX

considered as the best-performing and efficient electrolyte that has been more or less established due to the very fast regeneration of the dye combining with the redox couple I^-/I_3^-. However, a large volume of the recent works on DSSCs is devoted to the substitution of this redox couple with alternative materials.[14−17] This is mainly due to some disadvantages that the presence of I^-/I_3^- provokes: (a) this couple is highly corrosive and is thus destructive to metals (Ag, Au, Cu), which are used mainly as counter electrodes and metal grids in modules; (b) it absorbs visible light, reducing the photocurrent and consequently the power efficiency; and (c) the redox potential of the couple is not customized well; that is, the open circuit potential V_{oc} ranges to 0.7−0.8 V.[18−20] There is therefore a need to optimize the cells and to develop alternative charge-transport and regeneration systems, to replace iodide with a more transparent and less corrosive redox couple. Several attempts have been made to find a suitable alternative to the I^-/I_3^- system, including transition metal complexes.[21−24] However, these redox couples should exhibit improved physical and chemical properties such as good solubility, substantially optically clear at concentrations permitting good conductivity, high thermal stability, and finally noncorrosive toward the components of the solar cell. Besides, in the conventional solar cell based on the I^-/I_3^- system, optimized efficiency was hampered due to the need of high driving force (~500 mV) for the regeneration of oxidized dye by I^-/I_3^- couple. This loss represents a strong limitation in the attainable open-circuit voltage of the cell and hence the photovoltaic performance of the cell. For this reason, the development of alternative redox mediators should further improve the technology of DSSCs. Recently, the cobalt(II/III) complexes $[Co^{III/II}(ttcn)_2]^{3+/2+}$ and $[Co^{III/II}(bpy)_3]^{3+/2+}$ with the ligands trithiacyclononane (ttcn)[25] and 2,2′-bipyrine (bpy),[26] respectively, have been used in DSSCs as efficient redox couples. DSSCs with 13% efficiency were achieved through the molecular engineering of porphyrin sensitizers.[27] It is worth noting that one of the major advantages of using transition metal complexes as redox couples in DSSCs is that their redox potentials can be tuned by modifying the ligands, as distinguished from the I^-/I_3^- system. Furthermore, the ligand properties can be tuned so as to modulate the relative activation energies for electron-transfer processes involving the metal complexes.[28,29] In addition to the use of cobalt(II/III) complexes as efficient redox mediators, several other organometallic compounds were proposed as alternatives to the I^-/I_3^- electrolytes such as ferrocene/ferrocenium[30] (Fc/Fc^+), nickel(III/IV)[31] $[Ni^{III/IV}(dicarbollide)_2]^{0/-1}$, and very recently the oxidovanadium(IV/V)[11] couple $[VO(salen)]^{0/+}$ [salen = *N*,*N*′-ethylenebis(salicylideneiminate)(2−)].

Herein, the syntheses and physicochemical characterization of the square pyramidal oxidovanadium(IV/V) complexes $(Ph_4P)_2[V^{IV}O(hybeb)]$ and $Ph_4P[V^{V}O(hybeb)]$ are reported (Scheme 1), where $hybeb^{4-}$ is a tetradentate diamidodiphenolate(4−) ligand. The redox potential of the couple $[V^{IV}O(hybeb)]^{2-}/[V^{V}O(hybeb)]^-$ and the energy of highest occupied molecular orbital (HOMO) of the sensitizing dye and the HOMO of $[V^{IV}O(hybeb)]^{2-}$ were calculated by means of density functional theory (DFT) electronic structure calculation methods.

Moreover, the oxidovanadium(IV) complex $(Ph_4P)_2[V^{IV}O(hybeb)]$ was combined with its oxidized analogue $Ph_4P[V^{V}O(hybeb)]$ and applied as redox couple in the electrolyte of DSSCs. Their output and electrical efficiency were tested. To the best of our knowledge, it is only the second time that vanadium complexes are referred to as alternative redox mediators in DSSCs.[11]

Scheme 1. Chemical Structure of the Oxidovanadium(IV/V) Complexes

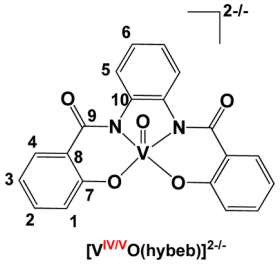

$[V^{IV/V}O(hybeb)]^{2-/-}$

EXPERIMENTAL SECTION

Materials. All chemicals were bought from Merck. Acetylsalicyloyl chloride and tetraphenylphosphonium chloride were used as received. 1,2-phenylenediamine was purified by sublimation. $[V^{IV}O(acac)_2]$,[32] $Na_2[VO(hybeb)]\cdot 3CH_3OH$ ($\mathbf{1}\cdot 3CH_3OH$),[33] and $Na[VO(hybeb)]\cdot CH_3OH$ ($\mathbf{2}\cdot CH_3OH$)[33] were prepared by the literature procedures or slight modifications of them (for the preparation of compounds $\mathbf{1}\cdot 3CH_3OH$ and $\mathbf{2}\cdot CH_3OH$ see Supporting Information). Dichloromethane and acetonitrile were dried and distilled over calcium hydride, while tetrahydrofuran was dried and distilled over sodium wire. All the solvents were distilled just prior to their use. Syntheses, distillations, crystallization of the complexes, and physicochemical characterizations were performed under high-purity argon using standard Schlenk techniques. C, H, and N analyses were conducted by the University of Hamburg microanalytical service; vanadium was determined gravimetrically as vanadium pentoxide or by atomic absorption.

Chloroplatinic acid hexahydrate, $[H_2Pt^{IV}Cl_6]\cdot 6H_2O$, was purchased from Sigma-Aldrich and used as received. Ruthenium(II) bis(tetrabutylammonium), N719, was purchased from Solaronix S.A, Switzerland. SnO_2:F transparent conductive electrodes (FTO, TEC A8) 8 Ohm/square were purchased from the Pilkington NSG Group. Commercial titanium isopropoxide (TTIP, 97%, Aldrich), Triton X-100 (polyethylene glycol *p*-*tert*-octylphenyl ether) surfactant (99.8%, Fisher Scientific), and glacial acetic acid (Aldrich) were used to make precursor TiO_2 sols. Titania powder P25 was provided by Degussa (Germany; 30% rutile and 70% anatase).

1,2-Bis(2-acetoxybenzamido)benzene (H_2hybebe). To a stirred anhydrous tetrahydrofuran (60 mL) solution of 1,2-phenylenediamine (2.722 g, 25.17 mmol) was added solid acetylsalicyloyl chloride (10.000 g, 50.34 mmol) in one portion under high-purity argon. The mixture was stirred for 18 h, and then water (300 mL) was added dropwise to the stirred suspension. The suspension was cleared after the addition of ~30 mL of water, and then further addition of water (270 mL) resulted in the formation of a white precipitate. The resulting precipitate was filtered off, washed with water (3 × 50 mL), and dried in vacuum. Yield: 8.70 g (80%). Anal. Calcd for $C_{24}H_{20}N_2O_6$ (M_r = 432.19): C, 66.66; H, 4.66; N, 6.48. Found: C, 66.70; H, 4.58; N, 6.50%.

1,2-Bis(2-hydroxybenzamido)benzene (H_4hybeb·0.6CH_3NO_2). H_2hybebe (2.350 g, 5.44 mmol) was dissolved in acetone (25 mL) at ambient temperature (~20 °C), and an aqueous solution of sodium hydroxide (12 mL, 6 M) was added dropwise (~5 min) under magnetic stirring. Then, the solution was cooled to ~0 °C, and concentrated (~12 M) hydrochloric acid (11 mL, ~48 mmol) was added dropwise to the stirred solution under magnetic stirring. The final pH value of the solution was ~1. The resulting white precipitate was filtered off and washed with water (2 × 50 mL). Yield: 1.88 g (99%). The product was recrystallized from nitromethane[34] (30 mL) to obtain off-white crystals of $H_4hybeb\cdot 0.6CH_3NO_2$. Yield after recrystallization: 1.450 g (77%). Anal. Calcd for $C_{20.6}H_{17.8}N_{2.6}O_{5.2}$ (M_r = 384.78): C, 64.25; H, 4.66; N, 9.46. Found: C, 64.30; H, 4.62; N, 9.51%. ^{1}H NMR (500 MHz; CD_3CN, ppm): δ 7.80 (dd, J = 7.9, 1.2 Hz, 2H), 7.68 (dd, J = 6.2, 3.2 Hz, 2H), 7.46 (dt, J = 7.9, 2.3 Hz, 2H), 7.37 (dd, J = 6.2, 3.2 Hz,

DOI: 10.1021/acs.inorgchem.5b00159
Inorg. Chem. XXXX, XXX, XXX−XXX

2H), 6.97 (m, 2H) and 6.95 (m, 2H), 4.31 (s) for $C\mathbf{H}_3NO_2$. ^{13}C NMR (500 MHz; CD_3CN, ppm): δ 161.5 C(7), 169.4 C(9), 135.1 C(2), 131.9 C(10′), 131.4 C(10), 128.4 C(4), 127.4 C(6), 127.1 C(5), 120.0 C(3), 118.9 C(1), 115.9 C(8′), 115.6 C(8), 63.51 (s) for $\mathbf{C}H_3NO_2$ (see Scheme 1 for atomic numbering).

Bis[tetraphenylphosphonium] [1-(2-hydroxybenzamido)-2-(2-pyridinecarboxamido)benzenato]oxidovanadate(IV), $(Ph_4P)_2[V^{IV}O(hybeb)]\cdot 0.8CH_2Cl_2$ ($\mathbf{3}\cdot 0.8CH_2Cl_2$). To a stirred suspension of $Na_2[VO(hybeb)]\cdot 3CH_3OH$ (0.500 g, 0.94 mmol) in CH_2Cl_2 (20 mL) was added in one portion solid Ph_4PCl (0.673 g, 1.88 mmol). The mixture was stirred for 3.0 h, under rigorous exclusion of oxygen. The complex dissolved, and a white solid (NaCl) separated. After filtration and concentration of the solution to ∼3 mL, the complex was precipitated by adding dropwise and with stirring 10 mL of diethyl ether. The resulting pale green precipitate was filtered off, washed with diethyl ether (2 × 10 mL), and dried in vacuo. Yield: 0.816 g (75%). High-resolution electrospray ionization mass spectrometry (HR-ESI(−)-MS): calcd for $C_{20}H_{12}O_5N_2V$ ($[M]^{-2}$) 205.5145, 205.5198 found. Anal. Calcd for $C_{68.8}H_{53.6}Cl_{1.6}N_2P_2O_5V$ (M_r = 1157.32): C, 71.34; H, 4.67; N, 2.42; V, 4.40. Found: C, 70.95; H, 4.70; N, 2.36; V, 4.41%.

Tetraphenylphosphonium [1,2-bis(2-hydroxybenzamido)-benzenato]-oxidovanadate(V), $Ph_4P[V^{V}O(hybeb)]\cdot 0.3CH_2Cl_2$ ($\mathbf{4}\cdot 0.3CH_2Cl_2$). The complex was prepared in a fashion similar to that used for complex $\mathbf{3}\cdot 0.8CH_2Cl_2$ except that 1 equiv of Ph_4PCl was used to get $\mathbf{4}\cdot 0.3CH_2Cl_2$ in 67% yield. HR-ESI(−)-MS: calcd for $C_{20}H_{12}O_5N_2V$ ($[M]^{-}$) 411.0180, 411.0147 found. Anal. Calcd for $C_{44.3}H_{32.6}Cl_{0.6}N_2O_5PV$ (M_r = 775.70): C, 68.54; H, 4.24; N, 3.61, V, 6.57. Found: C, 68.31; H, 4.30; N, 3.70; V, 6.60%.

Electron Paramagnetic Resonance Spectroscopy. The continuous wave X-band electron paramagnetic resonance (EPR) spectra of the compounds were acquired on an ELEXSYS E500 Bruker spectrometer at a resonance frequency of ∼9.5 GHz and a modulation frequency of 100 MHz. For the full EPR spectra (ΔB = 100 mT, 3000 points), 20 scans were accumulated. The optimization of the spin Hamiltonian parameters and EPR data simulation were performed by using the software package easy spin 4.5.5.[35]

Preparation of TiO_2 Photoanodes Sensitized with N719 Dye. TiO_2 thin films were first deposited on fluorine-doped tin oxide (FTO) glasses as blocking layers, following a previously reported procedure.[36,37] Briefly, for 5.4 mL of solution, 0.72 g of Triton X-100 were mixed with 4 mL of ethanol, followed by addition of 0.4 mL of glacial acetic acid and 0.32 mL of titanium(IV) isopropoxide under vigorous stirring. After this solution was stirred for a few minutes, FTO glasses were dipped in the above solution and withdrawn at rate of 2 cm/sec. The films were heated to 500 °C for 30 min using a 20 °C/min heating ramp rate. The procedure was applied for the deposition of only one TiO_2 layer; the film thickness was ∼150 nm. Then, a layer of TiO_2 paste was deposited by doctor blading followed by heating to 500 °C. The fabrication of TiO_2 paste is as follows: 3 g of TiO_2-Degussa P25 was mixed with 0.5 mL of acetic acid in a mortar for ∼3 min. Thereafter, 2.5 mL of Millipore water and 17.5 mL of ethanol were alternately added to break all TiO_2 aggregates and form a homogeneous solution. The solution was transferred to a crucible with 50 mL of ethanol and was mixed with 10 g of terpineol and an amount of ethyl cellulose. The solution was ultrasonicated for ∼2 min, and then the crucible was placed in a rotary evaporator at 40−45 °C to remove the excessive solvent and form the TiO_2 paste. The TiO_2 films have a total thickness of ∼5 μm and were prepared by the previously described procedure and immersed into a 5×10^{-4} M (ethanol/acetonitrile 50:50) solution of N719 dye overnight to complete the photoanode preparation. However, note that thicker TiO_2 films might improve efficiency of the cells. Excessive dye molecules that were not adsorbed on the TiO_2 surface were removed by rinsing with acetonitrile.

Vanadium Electrolyte Preparation. In the construction of the solar cell, a liquid electrolyte based on vanadium redox couple was used. The composition of the first electrolyte is as follows: 0.05 M of the vanadium(IV) complex $(Ph_4P)_2[V^{IV}O(hybeb)]$ and 0.005 M of the vanadium(V) complex $Ph_4P[V^{V}O(hybeb)]$ were diluted in acetonitrile. After this solution was stirred for 6 h, one drop of each electrolyte was placed on the top of the titania electrode with adsorbed dye molecules, and a slightly platinized FTO counter electrode was pushed by hand on the top. The platinized FTO glass was made by casting a few drops of a solution of $[H_2Pt^{IV}Cl_6]\cdot 6H_2O$ (5 mg/mL of ethanol) followed by heating at 500 °C for 10 min.

Electrochemistry. Cyclic voltammetry (CV) and rotating disk experiments were conducted on an EG&G Princeton Applied Research 273A potentiostat/galvanostat. Electrochemical procedures were performed with a three-electrode configuration: a platinum disk electrode (surface area of 0.13 mm^2) was used as the working electrode, and a platinum wire was used as the auxiliary electrode and as reference. Excess of electrolyte (0.9 M tetrabutylammonium perchlorate (TBAP)) was added to minimize ohmic resistance. The potential was calibrated using ferrocene as internal standard (0.63 V vs normal hydrogen electrode (NHE)).[38] The diffusion coefficient D was calculated by Levich's equation.[39]

The heterogeneous electron-transfer rate constant k_0 (cm s^{-1}) for the electrode reaction was determined by Nicholson's equation, using the D value calculated from Levich's equation.[39]

Impedance measurements of the as-prepared solar cells based on the aforementioned complexes were performed under solar light illumination provided from a Xe light source using a Solar Light Co. solar simulator (model 16S-300) equipped with AM0 and AM 1.5 direct Air Mass filters to simulate solar radiation at the surface of the Earth. In particular, electrochemical impedance spectroscopy (EIS) measurements were performed with Metrohm Autolab 3.v potentiostat galvanostat (model PGSTAT 128N) through a frequency range from 100 kHz to 0.01 Hz, using a perturbation of ±10 mV over the open-circuit potential. Experimental data are presented by scattering symbols, while lines represent the fitted plots obtained using Nova 1.10 software.

Nuclear Magnetic Resonance Measurements. Samples were prepared by diluting a proper amount of compound in 0.600 mL MeCN-d_3 in a 5 mm NMR tube. NMR Spectra were recorded in a Bruker AV 500 MHz instrument. The ^{51}V spectrum was recorded at 105.32 MHz using a spectral width of 720 ppm with 16 000 data points, 90° pulse, a relaxation delay of 0.5 s, and an acquisition time of 0.1 s. A 3 Hz line broadening was applied prior to the Fourier transformation. The chemical shifts are reported with respect to $V^{V}OCl_3$ at 0 ppm.

Characterization of the Dye-Sensitized Solar Cells. For the current density−voltage ($J-V$) curves, the samples were illuminated with Xe light using a Solar Light Co. solar simulator (model 16S-300) equipped with AM 0 and AM 1.5 direct Air Mass filters to simulate solar radiation at the surface of the Earth. The light intensity was kept constant at 1000 W/m^2 measured with a CMP 3 Kipp & Zonen pyranometer. Finally, the current−voltage ($I-V$) curves were recorded by connecting the cells to a Keithley Source Meter (model 2601A), which was controlled by Keithley computer software (LabTracer). The cell active area was constant at 2 cm^2, while mask of 0.3 cm^2 was used in all measurements. For each case, we made three devices, which were tested under the same conditions to avoid any misleading estimation of their efficiency. Cell performance parameters, including short-circuit current (I_{SC}), open-circuit voltage (V_{OC}), maximum power (P_{max}), fill factor (FF), and overall cell conversion efficiency, were measured and calculated from each $J-V$ characteristic curve.

Computational Details. All calculations were performed using the Gaussian 09 program suite.[40] The geometries of the oxidovanadium(IV/V) complexes were fully optimized, without symmetry constraints, employing the 1997 hybrid functional of Perdew, Burke, and Ernzerhof[41] as implemented in the Gaussian09 program suite. This functional uses 25% exchange and 75% correlation weighting and is denoted as PBE0. For the geometry optimizations, we used the Def2-TZVP basis for all atoms. Hereafter the method used in DFT calculations is abbreviated as PBE0/Def2-TZVP. All stationary points were identified as minima (number of imaginary frequencies N_{imag} = 0). Acetonitrile solvent effects were taken into account with the polarizable continuum model (PCM) using the integral equation formalism variant (IEFPCM) being the default self-consistent reaction field (SCRF) method.[42] The energies of the frontier MOs of the N719 Ru dye were obtained from a single-point energy calculation in CH_3CN solution (PCM model) at the PBE0/Def2-TZVP using the X-ray structure of the dye.[43]

DOI: 10.1021/acs.inorgchem.5b00159
Inorg. Chem. XXXX, XXX, XXX−XXX

RESULTS AND DISCUSSION

Syntheses. The organic molecules H_2hybebe and H_4hybeb·0.6 CH_3NO_2 were prepared by modifications of the reported literature procedures.[33] In particular, H_4hybeb·0.6CH_3NO_2 was synthesized with substantial modifications of the literature-reported synthesis[33] to increase the yield and to reduce the time of the synthesis (5 min vs 12 h). The sodium ions of the oxidovanadium(IV/V) compounds **1**·3CH_3OH and **2**·CH_3OH were substituted for tetraphenylphosphonium counterions to increase their solubility and their hydrolytic stability in acetonitrile. High purity of $[V^{IV}O(acac)_2]$[44] and H_4hybeb·0.6 CH_3NO_2 was essential for the preparation of **1**·3CH_3OH.

Electron Paramagnetic Resonance Spectroscopy. The EPR spectrum of the oxidovanadium(IV) compound **3**·0.8 CH_2Cl_2 in acetonitrile solution gave the characteristic eight-line isotropic spectrum (Figure 1) at room temperature (RT) and the 16-line anisotropic spectrum (Figure 2) at 120 K.

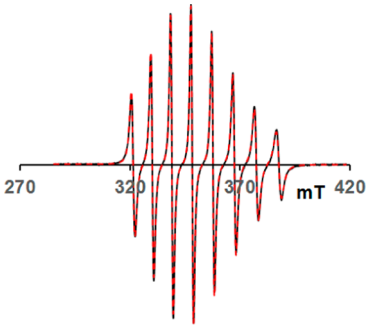

Figure 1. X-Band EPR spectrum of compound **3**·0.8CH_2Cl_2 in dried CH_3CN solution (7.00 mM) at RT (black line) and its simulated spectrum (red dashed line).

The *g*- and *A*-EPR parameters of the anisotropic spectrum of **3**·0.8 CH_2Cl_2 (Table 1) were calculated by simulation of its anisotropic experimental spectrum (Figure 2). These parameters are close to those reported[33] for the Na^+ salt of $[V^{IV}O(hybeb)]^{2-}$ ($g_\perp$= 1.978, $g_\parallel$ = 1.960, $A_\perp$= −53.6 × 10^{-4} cm^{-1} and $A_\parallel$ = −156.2 × 10^{-4} cm^{-1} and A_0 = 87.8 × 10^{-4} cm^{-1}).

However, partial aerial oxidation (i.e., in the solution coexist V^{IV} and V^V species) of the compound **3**·0.8CH_2Cl_2 in CH_3CN solution (containing 1% H_2O) gave peaks from an additional species (Table 1). The simulation of this spectrum (Figure 2B) resulted in larger hyperfine splitting and a shift to lower *g* values for the new species in comparison to those of $[V^{IV}O(hybeb)]^{2-}$. The new species was assigned to the oxidovanadium(IV) compound with a protonated phenolic oxygen (Scheme 2).

The protonation of the phenolic oxygen, according to the additivity rule,[45] increases the $A_\parallel$ to ∼10 × 10^{-4} cm^{-1}, which is the same as the observed increment by the experiment. The formation of either V^{IV}=O···V^V=O or O=V^{IV}−O−V^V=O dinuclear adduct should be excluded because such complexes are expected to exhibit higher *g* values and smaller hyperfine splitting.[46] In addition, any ligation to the sixth axial empty position of $[V^{IV}O(hybeb)]^{2-}$ is excluded because it would result in a smaller orbital splitting, depopulation of the d_{xy} orbital and thus smaller hyperfine splitting.[45d,47] Electrochemistry and UV−vis experiments have shown that the species $[V^{IV}O(hybeb)]^{2-}$ retains the square pyramidal geometry in strong donating solvents.[28]

Although the complex anion $[V^{IV}O(hybeb)]^{2-}$ is stable in solution toward hydrolysis, it can be easily oxidized to its

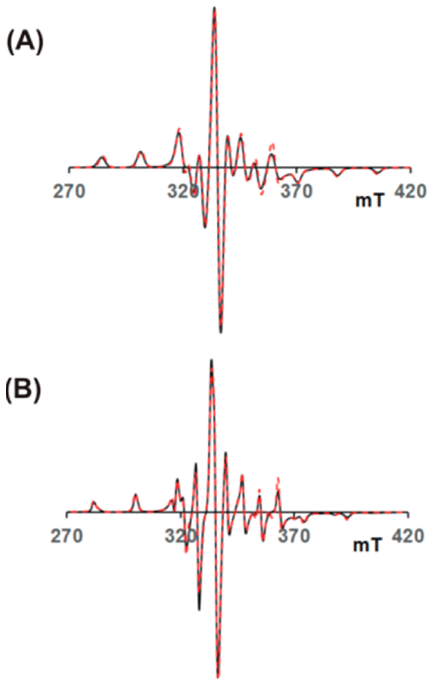

Figure 2. (A) X-band EPR spectrum of a frozen solution of the compound **3**·0.8CH_2Cl_2 in dried CH_3CN (7.00 mM) at 120 K (black line) and the simulated spectrum (red dashed line). (B) X-band EPR spectrum of a frozen CH_3CN solution (containing 1% H_2O) of **3**·0.8CH_2Cl_2 (2.59 mM), which had been partially oxidized by bubbling air for 1 h into it, at 120 K (black line) and the simulated spectrum (red dashed line) obtained using $g_\perp$= 1.980, $g_\parallel$ = 1.954, $A_\perp$= −50.8 × 10^{-4} cm^{-1} and $A_\parallel$ = −158.6 × 10^{-4} cm^{-1} for $[V^{IV}O(hybeb)]^{2-}$ (21%) and $g_\perp$= 1.975, $g_\parallel$ = 1.942, $A_\perp$= −60.1 × 10^{-4} cm^{-1} and $A_\parallel$ = −168.6 × 10^{-4} cm^{-1} for the new species (79%).

oxidovanadium(V) analogue $[V^VO(hybeb)]^-$, which is sensitive to hydrolysis, and it is hydrolyzed releasing protons to the solution; these protons protonate the phenolic oxygen atom of $[V^{IV}O(hybeb)]^{2-}$ species (Scheme 2).

This is also supported by the HR-ESI(−)-MS (in methyl alcohol not dried; Figure 3) and ^{51}V NMR (in CD_3CN not dried) spectra of $Ph_4P[V^VO(hybeb)]$·0.3 CH_2Cl_2.

In Figure 4 are shown the EPR spectra of $(Ph_4P)_2[V^{IV}O$-$(hybeb)]$·0.8CH_2Cl_2 and of various mixtures of this species with its oxidized counterpart $Ph_4P[V^VO(hybeb)]$·0.3CH_2Cl_2 in dried CH_3CN at room temperature.

In dried CH_3CN, the hydrolysis of the complex anion $[V^VO(hybeb)]^-$ does not take place, and thus, the complex anion $[V^{IV}O(\mathbf{H}hybeb)]^-$ is undetectable by EPR spectroscopy (vide supra). Clearly, in dried CH_3CN and rigorous exclusion of oxygen both oxidovanadium(IV/V) complexes are stable. The observed rate constant of the electron transfer k_{obs} between the oxidovanadium(IV/V) complexes $[V^{IV}O(hybeb)]^{2-}$ and $[V^VO$-$(hybeb)]^-$ was determined from the EPR line-width broadening of the eight peaks of the oxidovanadium(IV) signal, at room temperature, according to eq 1.

$$k_{obs} = 3^{1/2}\pi\gamma_e(\Delta B - \Delta B^0)/\{(1 - p_i)([V^VO(hybeb)^-]\} \quad (1)$$

where γ_e is the gyromagnetic ratio of the electron (γ_e = 2.803 × 10^7 mT^{-1} s^{-1}), p_i is the statistical population factor of the EPR line *i*, and ΔB^0 and ΔB are the line widths calculated from the simulation of the spectra (Figure 5) in the absence and presence of the self-exchange broadening, respectively.[11,45e] Using p_i =

DOI: 10.1021/acs.inorgchem.5b00159
Inorg. Chem. XXXX, XXX, XXX−XXX

Table 1. EPR Parameters of the Oxidovanadium(IV) Complexes $[V^{IV}O(hybeb)]^{2-}$ and Its Protonated Analogue $[V^{IV}O(Hhybeb)]^{-}$

complex	$g_\perp$	$g_\parallel$	$A_\perp \times 10^{-4}$, cm^{-1}	$A_\parallel \times 10^{-4}$, cm^{-1}	g_0	$A_0 \times 10^{-4}$, cm^{-1}
$[V^{IV}O(hybeb)]^{2-}$	1.980	1.954	−50.8	−158.6	1.975	87.3
$[V^{IV}O(Hhybeb)]^{-}$	1.975	1.942	−60.1	−168.6	1.967	96.8

Scheme 2. Possible Mechanism of the Protonation of the Complex Anion $[V^{IV}O(hybeb)]^{2-}$ Leading to $[V^{IV}O(Hhybeb)]^{-}$ through Hydrolysis of $[V^{V}O(hybeb)]^{-}$

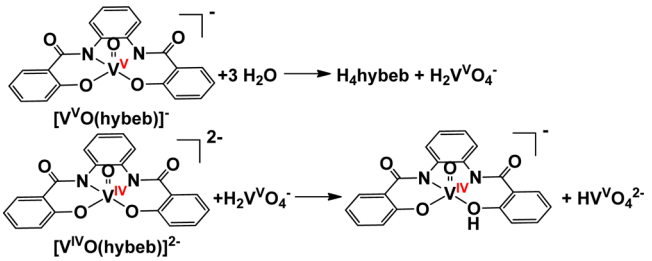

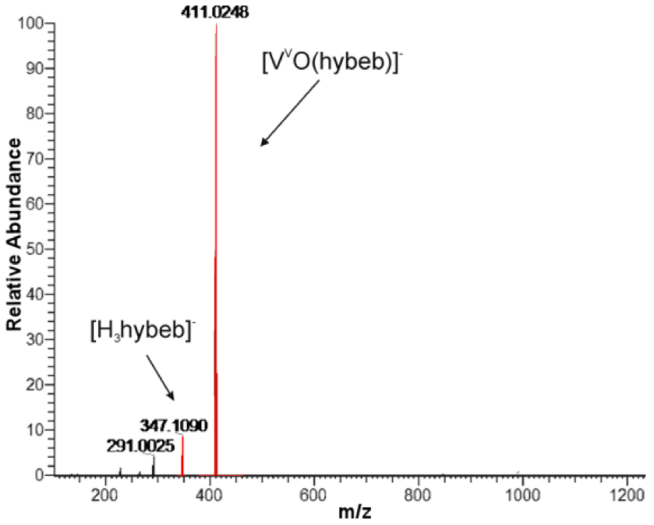

Figure 3. HR-ESI negative mass spectrum of $Ph_4P[V^{V}O(hybeb)]\cdot 0.3CH_2Cl_2$ in methyl alcohol (not dried), showing isotopic distribution envelopes of $[V^{V}O(hybeb)]^{-}$ and $[H_3hybeb]^{-}$ centered at m/z = 411.0147 and 347.1090, respectively.

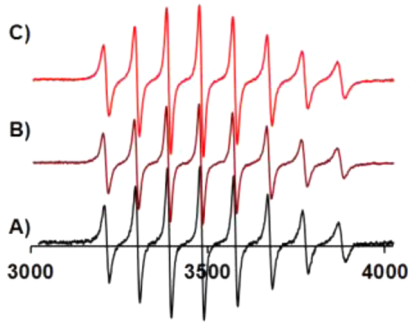

Figure 4. X-Band EPR spectra of an acetonitrile solution, at RT, of (A) $(Ph_4P)_2[V^{IV}O(hybeb)]\cdot 0.8CH_2Cl_2$ (1.22 mM) (black line), (B) $(Ph_4P)_2[V^{IV}O(hybeb)]\cdot 0.8CH_2Cl_2$ (1.22 mM) and $Ph_4P[V^{V}O(hybeb)]\cdot 0.3CH_2Cl_2$ (0.593 mM) (brown line), and (C) $(Ph_4P)_2[V^{IV}O(hybeb)]\cdot 0.8CH_2Cl_2$(1.22 mM) and $Ph_4P[V^{V}O(hybeb)]\cdot 0.3CH_2Cl_2$ (4.74 mM) (red line).

0.13 and correcting the exchange rate of the couple $[V^{IV}O(hybeb)]^{2-}/[V^{V}O(hybeb)]^{-}$ using eq 2

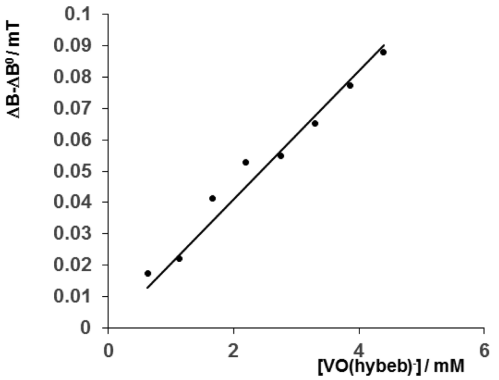

Figure 5. Plot of changes in the line width for the EPR signals found from the simulation of the experimental EPR spectra in mT vs the concentration of $[V^{V}O(hybeb)]^{-}$.

$$1/k_{ex} = 1/k_{obs} - 2/k_{diff} \quad (2)$$

where $k_{diff} = (8RT/3\eta)$, the exchange rate for the $[V^{IV}O(hybeb)]^{2-}/[V^{V}O(hybeb)]^{-}$ couple was found to be $k_{ex} = 3.9 \times 10^9$ M^{-1} s^{-1}, which is less than the rate constant observed for the $[V^{IV}O(salen)]^{0}/[V^{V}O(salen)]^{+}$ couple ($k_{ex} = 7.4 \times 10^9$ M^{-1} s^{-1}) but much higher than that reported for the nitroxide radicals such as TEMPO$^{0/+}$ (2.7×10^7 M^{-1} s^{-1}),[48] which typically has been attributed to an outer-sphere exchange mechanism. At this point, it is worth noting that the k_{ex} of the nonoxidovanadium(IV/V) species[49a] $[V^{IV/V}(hidpa)_2]^{2-/-}$ is ~1×10^5 M^{-1} s^{-1}, while the k_{ex} of the redox couple[49b] *cis*-$[V^{IV}O(OH)(bpy)_2]^{+}/[V^{V}O_2(bpy)_2]^{+}$ is $(1.0 \pm 0.3) \times 10^{-1}$ M^{-1} s^{-1}.

Electrochemistry. The CV study of $3\cdot 0.8CH_2Cl_2$ in CH_3CN solution (1.00 mM) reveals one reversible $[V^{IV}O(hybeb)]^{2-}/[V^{V}O(hybeb)]^{-}$ redox wave at −0.047 V vs NHE. The CV study of $4\cdot 0.3CH_2Cl_2$ (the oxidized analogue of $3\cdot 0.8CH_2Cl_2$) in CH_3CN solution provided results identical to those for $3\cdot 0.8CH_2Cl_2$. The cyclic voltammograms of compound $3\cdot 0.8CH_2Cl_2$ in CH_3CN at various scan rates (Figure 6) show one electron reversible electron transfer; $i_a/v^{1/2}$ and $E_{1/2}$ are independent of the scan rate (v) and $i_a/i_c = 1$, where i_a and i_c are

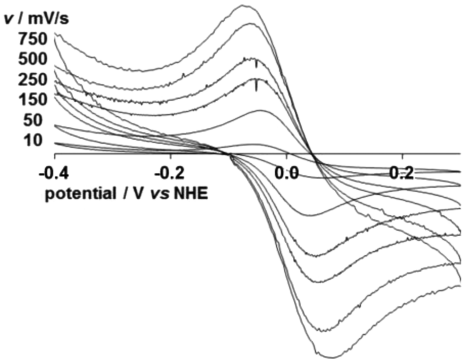

Figure 6. Cyclic voltammograms of compound $3\cdot 0.8\ CH_2Cl_2$ in dried CH_3CN solution (1.00 mM), containing 0.9 M TBAP, recorded at various scan rates (v). The data were used for the calculation of the heterogeneous electron transfer rate constant $k_0 = 7.7 \times 10^{-3}$ cm s^{-1}.

DOI: 10.1021/acs.inorgchem.5b00159
Inorg. Chem. XXXX, XXX, XXX−XXX

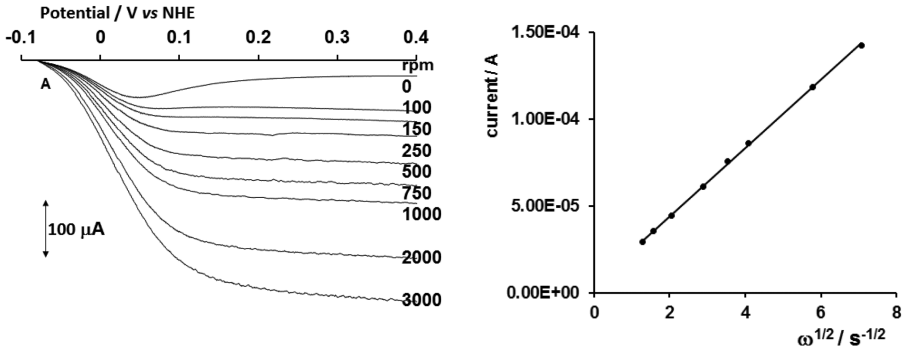

Figure 7. (A) Current−potential curves obtained with a rotated disk electrode of compound **3**·0.8CH_2Cl_2 in CH_3CN solution (1.00 mM) containing 0.9 M $^tBu_4NClO_4$ as supporting electrolyte; at scan rate 10 mV s^{-1}. (B) A plot of the diffusion limited currents vs the square root of the rotation rates of the electrode obtained from Figure 7A used for the determination of the diffusion coefficient $D = 1.0 \times 10^{-5}$ cm^2 s^{-1}.

the anodic and cathodic peak currents, respectively, and $\Delta E = E_a - E_b$ is close to 65 mV at low scan rates.

The potential−current curves of compound **3**·0.8CH_2Cl_2 in CH_3CN solution (1.00 mM) recorded at various rotation rates with a rotating disc working electrode are shown in Figure 7A. The diffusion coefficient D (1.0×10^{-5} cm^2 s^{-1}) for **3**·0.8CH_2Cl_2 was calculated from the Levich plot (Figure 7B) This plot is linear as a result of the electrochemical reversibility of the redox couple $[V^{IV}O(hybeb)]^{2-}/[V^{V}O(hybeb)]^{-}$. The D value found for **3**·0.8CH_2Cl_2 is similar to the D value for the compound $[V^{IV}O(salen)]$ (5.8×10^{-6} cm^2 s^{-1}).[11]

The heterogeneous electron transfer rate constant k_0 was estimated using the above D value and ΔE ($= E_a - E_b$) at various scan rates at CVs. The value of k_0 found for **3**·0.8CH_2Cl_2 (7.7×10^{-3} cm s^{-1}) is almost one-third of the corresponding value for the compound $[V^{IV}O(salen)]$ (2.7×10^{-2} cm s^{-1}). The electron transfer is rapid and reduces the electrode reaction-related cell resistance.

^{51}V Spectra of Compound 4·0.3 CH_2Cl_2. The ^{51}V spectrum of the oxidovanadium(V) compound $[Ph_4P]^+[V^{V}O(hybeb)]^-$ (**4**·0.3 CH_2Cl_2) in dry CD_3CN solution shows one resonance signal at −465 ppm with a half-height line width $\Delta\nu_{1/2}$ of 293 Hz. This chemical shift is the same as that observed for a CD_2Cl_2 solution of $[(Ph_3P)_2N]^+[V^{V}O(hybeb)]^-$ (**5**) {in which Ph_4P^+ was substituted for $[Ph_3P{=}N{=}PPh_3]^+$} indicating that the vanadium coordination environment in $[V^{V}O(hybeb)]^-$ is the same in both solvents.

On the basis of the heteroatom electronegativities tabulated by Zang,[50] we obtain $\sum\chi = 17.05$ for the complex $[V^{V}O(hybeb)]^-$ [$\sum\chi$ is the sum of the electronegativities of the three oxygen and two nitrogen atoms coordinated to vanadium(V)]. Applying these values to Rehder's[51] referencing scale, one predicts shift values in the upfield region between −400 and −500 ppm for a five-coordinate vanadium(V) compound. This is in agreement with the observed value of −465 ppm for the complex $[V^{V}O(hybeb)]^-$, and thus, the vanadium(V) atom most likely retains its coordination number in the CH_3CN solution.

^{13}C NMR Spectra of Compound 4·0.3 CH_2Cl_2. The carbon peaks of the CH_3CN solution of $[VO(hybeb)]^-$ at 132.43 C(8), 117.62 C(6), 127.1, 127.4, 128.4, and 120 ppm, obtained from the two-dimensional (2D) {^{1}H, ^{13}C} HSQC and the 2D {^{1}H, ^{13}C} HMBC spectra were assigned to the coordinated ligand. The stronger peaks at 135.1, 130.16, and 118.9 ppm belong to the Ph_4P^+ cation. The C(9)=O [167.0 (169.4 for the free ligand)] and the C(7)−O [164.6 (161.5 for the free ligand)] gave the largest shifts in comparison with those of the free ligand implying that the ligand hybeb^{4-} is bonded to vanadium through the two deprotonated amide nitrogen and two deprotonated phenolic oxygen donor atoms (Scheme 1).

Solar Cell Performance. The energy levels of the main components of the DSSC and the relative position of the redox potential for the complexes $(Ph_4P)_2[V^{IV}O(hybeb)]$ and (Ph_4P)-$[V^{V}O(hybeb)]$ according to the electrochemistry data are presented in Figure 8. Obviously, the relative position of this redox mediator is energetically lower than that referred to for the basic state of the N719 dye, and thus, it promotes the dye's regeneration in a successful way (see Figure 8). At this point, it is worth noting that the theory confirms this statement (vide infra), but although the SOMO of $[V^{IV}O(hybeb)]^{2-}$ is more positive than the HOMO of the N719 dye (see Figure 11), the energy difference is relatively small; thus, the driving force for dye regeneration should not be optimal.

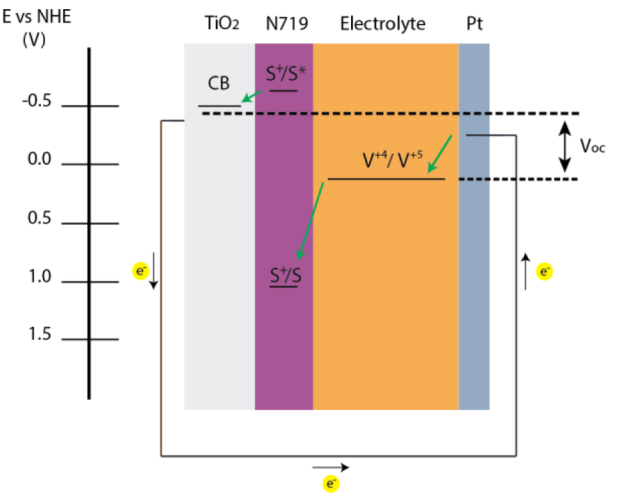

Figure 8. Redox potential for $(Ph_4P)_2[V^{IV}O(hybeb)]$ and (Ph_4P)-$[V^{V}O(hybeb)]$ mediators in relation to the energy levels of the dye/TiO_2 photoanode.

The $J-V$ typical curves were performed for several concentrations of $(Ph_4P)_2[V^{IV}O(hybeb)]$ and $(Ph_4P)[V^{V}O$-

DOI: 10.1021/acs.inorgchem.5b00159
Inorg. Chem. XXXX, XXX, XXX−XXX

(hybeb)] as redox mediators dissolved in dried acetonitrile. Initially, the two complexes were used separately as electrolytes solely dissolved in acetonitrile, but very poor results were finally obtained. Optimized results appear in Figure 9 where solar cells constructed with an electrolyte consisting of 0.05 M $(Ph_4P)_2[V^{IV}O(hybeb)]$ and 0.005 M $(Ph_4P)[V^{V}O(hybeb)]$ dissolved in acetonitrile were applied.

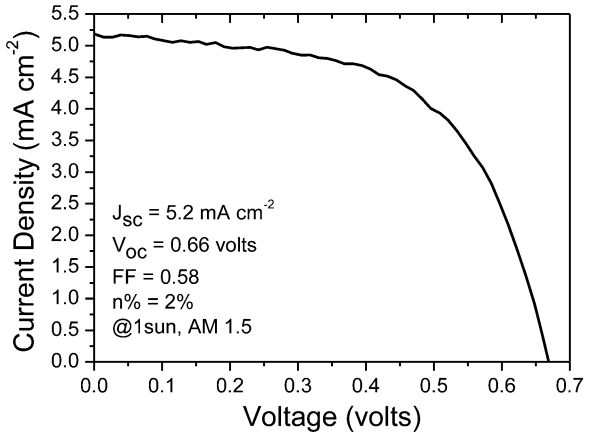

Figure 9. Characteristic current density (J) vs voltage (V) curve of the best-performing DSSC fabricated with an electrolyte based on the complexes $(Ph_4P)_2[V^{IV}O(hybeb)]$ and $(Ph_4P)[V^{V}O(hybeb)]$.

The highest energy conversion efficiency of 2% was achieved under simulated sunlight (AM 1.5, 1000 W/m^2), while lower quantities of the complexes showed lower values for J_{sc} and V_{oc}. However, higher amount of the complexes showed no remarkable changes to the short-circuit current densities and open-circuit voltages. It is noticeable that no electrolyte additives, such as lithium perchlorate or *tert*-butylpyridine, were applied for current or voltage enhancement. The obtained results refer to the use of a commercial dye (N719) as the most applicable sensitizer in DSSCs with standard potential for its reduced form. We recognize that the obtained efficiency could be even higher in case of the use of other pure organic dyes as recently better results were monitored for MK2 and D107 commercial dye products and cobalt-based redox mediators,[52,53] but our work is referred to the more stable and most-used dye in the literature.

The DSSCs were further characterized using electrochemical impedance spectroscopy (EIS). Figure 10 shows the Nyquist plot obtained from cells with optimized electrolyte composition. The first semicircle corresponds to the Pt/electrolyte interface, R_{pt}. The charge transfer resistance at the counter electrode (R_{pt}) is represented as a semicircle in the impedance spectra. The resistance element related to the response in the intermediate frequency represents the charge transport at the TiO_2/dye/electrolyte interface (R_{tr}) and shows diode-like behavior.

The equivalent circuits used to fit the experimental data are presented as inset in Figure 10. For electrodes having a rough surface the capacitance element (inset Figure 10) is replaced by a constant phase element (CPE, Q), which depends on the parameters Y_0 and N. It is possible to convert a CPE element, which is in parallel with a resistance, to a pseudo capacitance using eq 3. Finally, the intercept of the horizontal axis stands for the resistance of the sheet resistance of the FTO substrate and the contact resistance of the FTO/TiO_2 (R_h). The fitted parameters are summarized in Table 2.

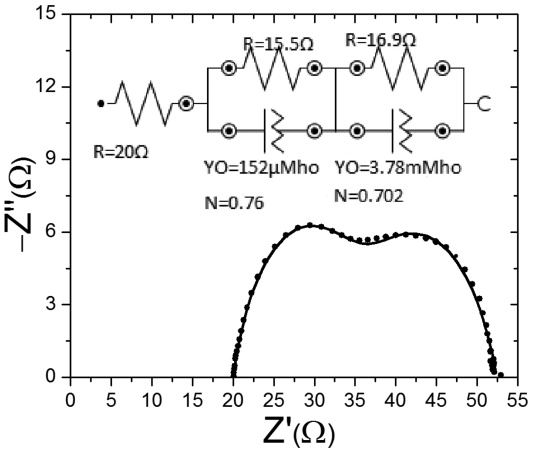

Figure 10. Impedance spectrum plot for optimized electrolyte composition at open-circuit voltage configuration irradiated with 1 sun solar light. (inset) DSSC equivalent circuit R(RQ)(RQ) used to fit the experimental data from the EIS measurements.

$$C_{pseudo} = Y_0^{(1/N)} R^{(1/N-1)} \quad (3)$$

The total series resistance of the cell can be calculated using eq 4. R_s was finally measured to be 35.5 Ω, which is a relatively low value for internal resistance of the cell based on liquid electrolyte.

$$R_S = R_h + R_{pt} \quad (4)$$

Computational Studies. The $[V^{IV}O(hybeb)]^{2-}/[V^{V}O(hybeb)]^{-}$ redox process has been studied by means of DFT electronic structure calculation methods.[54] The calculation of the redox potential for the following charge transfer reaction was based on the thermodynamic cycle shown in Scheme 3.

$$[V^{V}O(hybeb)]^{-}(soln.) + e^{-} \rightarrow [V^{IV}O(hybeb)]^{2-}(soln.) \quad (5)$$

The redox potential of reaction 5 in solution is related to the total change in the Gibbs free energy according to eq 6.[55]

$$E^{o} = -\Delta G^{o}_{soln.}/nF \quad (6)$$

where n is the number of electrons transferred ($n = 1$ in this case), F is the Faraday constant (equal to 23.061 kcal mol^{-1} V^{-1}), while $\Delta G^{o}_{soln.}$ is calculated from the thermodynamic cycle (Scheme 3) according to the following equation

$$\Delta G^{o}_{soln.} = \Delta G^{o}_{gas} + \Delta G^{o}[V^{V}O(hybeb)]^{-}_{soln.} - \Delta G^{o}[V^{IV}O(hybeb)]^{2-}_{soln.} \quad (7)$$

where ΔG^{o}_{gas} is the change of the standard Gibbs free energy of reaction 5 in the gas phase, while $\Delta G^{o}[V^{V}O(hybeb)]^{-}_{soln.}$ and $\Delta G^{o}[V^{IV}O(hybeb)]^{2-}_{soln.}$ are the standard free solvation energies of the $[V^{V}O(hybeb)]^{-}$ and $[V^{IV}O(hybeb)]^{2-}$species, respectively.

Using ΔG values, calculated at the PBE0/Def2-TZVP level of theory, for the Born−Haber thermodynamic cycle given in Scheme 3 and eq 6, we estimated the theoretical redox potential E^{o} of reaction 5 in solution to be equal to 4.43 V. On the basis of experimental and theoretical studies[56] the standard free energy for the standard process of formation of hydrogen from protons (eq 8) on the NHE is found to be equal to −4.36 V. Therefore, the redox potential of the couple $[V^{IV}O(hybeb)]^{2-}/[V^{V}O(hybeb)]^{-}$ versus NHE is −0.07 V in excellent agreement with the experimental value of −0.047 V.

DOI: 10.1021/acs.inorgchem.5b00159
Inorg. Chem. XXXX, XXX, XXX−XXX

Table 2. EIS Results of DSSC Fabricated with an Electrolyte Based on $(Ph_4P)_2[V^{IV}O(hybeb)]$ and $(Ph_4P)[V^{V}O(hybeb)]$ Complexes in Optimized Concentration

fitted parameters	R_h (Ω)	R_{pt} (Ω)	C_{pt} (× 10^{-4} F)	R_{tr} (Ω)	C_{tr} (× 10^{-3} F)
values	20.0 ± 0.1	15.5 ± 0.1	0.22 ± 0.01	16.9 ± 0.1	1.18 ± 0.01

Scheme 3. Thermodynamic Cycle Used to Calculate Gibbs Free Energies

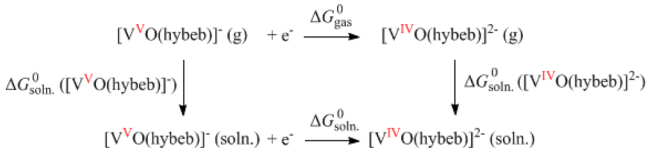

$$H^+(aq) + e^-(g) \rightarrow 1/2H_2(g) \quad (8)$$

One way to improve the efficiency of a DSSC[57] is to tune the regenerating electrolyte couple to the HOMO of the sensitizing dye to ultimately obtain a higher open-circuit voltage, V_{oc}. The HOMO of the sensitizing dye should lie below the energy level of the regenerating electrolyte couple or hole transporting material (HTM) so that after its oxidation upon electron injection to the conduction band of TiO_2 to be effectively regenerated by accepting electrons from the HTM.[58,59] The HOMOs of N719 dye and of $[V^{IV}O(hybeb)]^{2-}$, calculated at the PBE0/Def2-TZVP level augmented with the PCM solvation model for CH_3CN solution, are shown in Figure 11..

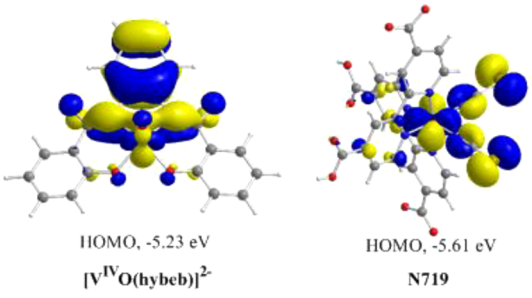

Figure 11. Three-dimensional contour plots of the HOMOs of $[V^{IV}O(hybeb)]^{2-}$and N719 dye in CH_3CN solution, at the PBE0/Def2-TZVP level.

Perusal of Figure 11 reveals that, although the HOMO of HTM is more positive than the HOMO of the N719 dye, the energy difference is relatively small, and thus, the driving force for dye regeneration should not be optimal. Notice that the HOMO of $[V^{IV}O(hybeb)]^{2-}$, which is involved in the oxidation process upon removal of an electron, is mainly located on one of the phenyls ring of the $hybeb^{4-}$ ligand as well as on the vanadium metal center.

Comparison of the Thermodynamic and Kinetic Parameters of the Oxidovanadium(IV/V) Complexes $[V^{IV/V}O(hybeb)]^{2-/-}$, $[V^{IV/V}O(salen)]^{0/+}$, and Iodide/Triiodide-Based Electrolytes. Many factors can affect the incident photon to charge carrier efficiency (IPCE) and $J-V$ behavior of DSSCs, making comparisons with literature results very difficult. In Table 3 are summarized the main thermodynamic and kinetic parameters of the oxidovanadium(IV/V) complexes $[V^{IV/V}O(hybeb)]^{2-/-}$, $[V^{IV/V}O(salen)]^{0/+}$, and iodide/triiodide-based electrolytes. The main difference between them is the $E_{1/2}$ of the redox couple $[V^{IV/V}O(hybeb)]^{2-/-}$, which is 0.49 and 0.63 V less positive than redox potential of $[V^{IV/V}O(salen)]^{0/+}$and I^-/I_3^-respectively. The other properties of the three electrolytes are very similar, and this means that the oxidovanadium(IV/V) redox couples can be potentially used as redox shuttles.

Table 3. Characteristics of $[V^{IV/V}O(hybeb)]^{2-/-}$, $[V^{IV/V}O(salen)]^{0/+}$, and Iodide/Triiodide-Based Electrolytes

electrolyte	$E_{1/2}$ [a]	k_{ex} [b] (× 10^9)	D [c]	k_0 [d]
$[V^{IV/V}O(hybeb)]^{2-/-}$	−0.047	3.9	1.0×10^{-5}	7.7×10^{-3}
$[V^{IV/V}O(salen)]^{0/+}$	0.44	7.4	5.8×10^{-6}	2.7×10^{-2}
I^-/I_3^-	0.58	23	7.6×10^{-6},[e]	5.3×10^{-3}

[a]In volts vs NHE. [b]Self-exchange rate constant in M^{-1} s^{-1}. [c]Diffusion coefficient in cm^2 s^{-1}. [d]The heterogeneous electron transfer rate constant in cm s^{-1}. [e]Reference 43.

CONCLUSIONS

In conclusion, the oxidovanadium(IV/V) complexes $(Ph_4P)_2[V^{IV}O(hybeb)]$ and $(Ph_4P)[V^{V}O(hybeb)]$ were synthesized and physicochemically characterized. The ideal properties of the complexes, including the large electron exchange and transfer rates and the reversible redox process resulting from EPR and electrochemistry, render the vanadium compounds suitable as candidates for redox mediators in DSSCs. The very large self-exchange rate constant offered an insight into the mechanism of the exchange reaction most likely mediated through an outer-sphere exchange mechanism. The redox couple $[V^{IV/V}O(hybeb)]^{2-/-}$, with a redox potential 0.63 V more negative than the I^-/I_3^-system, was successfully applied to iodide/iodine-free DSSCs sensitized with the ruthenium N-719 dye and yielded devices with efficiencies of 2% at 1 sun irradiation without the presence of any organic additive in the electrolyte.

The theoretical calculations revealed that the HOMO of $[V^{IV}O(hybeb)]^{2-}$, which is involved in the oxidation process upon removal of an electron, is more positive than the HOMO of the N719 dye, but this energy difference is relatively small; thus, the driving force for dye regeneration should not be optimal. The synthesis of suitable dye/$[V^{IV/V}O]^{2+/3+}$ redox mediators based on the theoretical calculations is underway in our laboratory to improve the solar cell efficiency.

ASSOCIATED CONTENT

Supporting Information

Experimental details for the synthesis of the compounds $Na_2[VO(hybeb)]\cdot 3CH_3OH$ ($\mathbf{1}\cdot 3CH_3OH$) and $Na[VO(hybeb)]\cdot CH_3OH$ ($\mathbf{2}\cdot CH_3OH$). This material is available free of charge via the Internet at http://pubs.acs.org.

AUTHOR INFORMATION

Corresponding Authors

*E-mail: attsipis@uoi.gr. (A.C.T.)
*E-mail:rehder@chemie.uni-hamburg.de. (D.R.)
*E-mail: tkampano@cc.uoi.gr. (T.A.K.)
*E-mail: akeramid@ucy.ac.cy. (A.D.K.)
*E-mail: estathatos@teiwest.gr. (E.S.)

Notes

The authors declare no competing financial interest.

DOI: 10.1021/acs.inorgchem.5b00159
Inorg. Chem. XXXX, XXX, XXX−XXX

■ ACKNOWLEDGMENTS

Prof. E. Stathatos acknowledges that his research has been cofinanced by the European Union (European Social Fund (ESF)) and Greek national funds through the Operational Program "Education and Lifelong Learning" of the National Strategic Reference Framework (NSRF) - Research Funding Program: ARCHIMEDES III, Investing in knowledge society through the ESF. We also thank the Research Promotional Foundation of Cyprus and the European Structural Funds for the purchase of EPR through ΑΝΑΒΑΘΜΙΣΗ/ΠΑΓΙΟ/0308/32 and Dr. C. Drouza for the EPR measurements. We are grateful to the Greek Community Support Framework III, Regional Operational Program of Epirus 2000-2006 (MIS 91629), for supporting the purchase of the LC-NMR cryoinstrument. The authors would like to thank the Unit of Environmental, Organic, and Biochemical high-resolution analysis-ORBITRAP-LC-MS of the Univ. of Ioannina for providing access to the facilities.

■ REFERENCES

(1) (a) Crans, D. C.; Smee, J. J. Vanadium. In *Comprehensive Coordination Chemistry II;* Elsevier Ltd: Amsterdam, The Netherlands, 2004; Vol. *4*, pp 175−239. (b) Crans, D. C.; Chatterjee, P. B. Vanadium Biochemistry. In *Comprehensive Inorganic Chemistry II: From Elements to Applications,* 2nd ed.; 2013; Vol. *3*, pp 323−342. (c) Yoshikawa, Y.; Sakurai, H.; Crans, D. C.; Micera, G.; Garribba, E. *Dalton Trans.* **2014**, *43*, 6965−6972. (d) Winter, P. W.; Al-Qatati, A.; Wolf-Ringwall, A. L.; Schoeberl, S.; Chatterjee, P. B.; Barisas, B. G.; Roess, D. A.; Crans, D. C. *Dalton Trans.* **2012**, *41*, 6419−6430. (e) Crans, D. C.; Trujillo, A. M.; Pharazyn, P. S.; Cohen, M. D. *Coord. Chem. Rev.* **2011**, *255*, 2178−2192. (f) Willsky, G. R.; Chi, L. H.; Godzala, M.; Kostyniak, P. J.; Smee, J. J.; Trujillo, A. M.; Alfano, J. A.; Ding, W.; Hu, Z.; Crans, D. C. *Coord. Chem. Rev.* **2011**, *255*, 2258−2269.

(2) (b) Rehder, D. *Met. Ions Life Sci.* **2013**, *13*, 139−169. (a) Rehder, D. *Future Med. Chem.* **2012**, *4*, 1823−1827.

(3) (a) Schneider, C. J.; Penner-Hahn, J. E.; Pecoraro, V. L. *J. Am. Chem. Soc.* **2008**, *130*, 2712−2713. (b) Schneider, C. J.; Zampella, G.; Greco, C.; Pecoraro, V. L.; De Gioia, L. *Eur. J. Inorg. Chem.* **2007**, 515−523.

(4) Rehder, D. *Dalton Trans.* **2013**, *42*, 11749−11761.

(5) Redshaw, C.; Tang, Y. *Chem. Soc. Rev.* **2012**, *41*, 4484−4510.

(6) (a) Sutradhar, M.; Shvydkiy, N. V.; Guedes da Silva, M. F. C.; Kirillova, M. V.; Kozlov, Y. N.; Pombeiro, A. J. L.; Shulpin, G. B. *Dalton Trans.* **2013**, *42*, 11791−11803. (b) Da Silva, J. A. L.; Fraústo da Silva, J. J. R.; Pombeiro, A. J. L. *Coord. Chem. Rev.* **2013**, *257*, 2388−2400.

(7) (a) Galloni, P.; Mancini, M.; Floris, B.; Conte, V. *Dalton Trans.* **2013**, *42*, 11963−11970. (b) Coletti, A.; Galloni, P.; Sartorel, A.; Conte, V.; Floris, B. *Catal. Today* **2012**, *192*, 44−55. (c) Coletti, A.; Whiteoak, C. J.; Conte, V.; Kleij, A. W. *ChemCatChem* **2012**, *4*, 1190−1196.

(8) (a) Maurya, M. R.; Bisht, M.; Kumar, A.; Kuznetsov, M. L.; Avecilla, F.; Pessoa, J. C. *Dalton Trans.* **2011**, *40*, 6968−6983. (b) Maurya, M. R.; Kumar, A.; Pessoa, J. C. *Coord. Chem. Rev.* **2011**, *255*, 2315−2344. (c) Maurya, M. R.; Haldar, C.; Kumar, A.; Kuznetsov, M. L.; Avecilla, F.; Costa Pessoa, J. *Dalton Trans.* **2013**, *42*, 11941−11962. (d) Pessoa, J. C.; Correia, I.; Adão, P. In *Advances in Organometallic Chemistry and Catalysis;* Pombeiro, A. J. L., Ed.; John Wiley & Sons: Hoboken, NJ, 2014; pp 227−232. (e) Maurya, M. R.; Chaudhary, N.; Avecilla, F.; Adaoc, P.; Pessoa, J. C. *Dalton Trans.* **2015**, *44*, 1211−1232.

(9) (a) Yamamoto, K.; Oyaizu, K.; Tsuchida, E. *J. Am. Chem. Soc.* **1996**, *118*, 12665. (b) Oyaizu, K.; Yamamoto, K.; Yoneda, K.; Tsuchida, E. *Inorg. Chem.* **1996**, *35*, 6634. (c) Tsuchida, E.; Oyaizu, K.; Dewi, E. L.; Imai, T.; Anson, F. C. *Inorg. Chem.* **1999**, *38*, 3704. (d) Bizzarri, C.; Conte, V.; Floris, B.; Galloni, P. *J. Phys. Org. Chem.* **2011**, *24*, 327−334. (e) Donakowski, M. D.; Gorne, A.; Vaughey, J. T.; Poeppelmeier, K. R. *J. Am. Chem. Soc.* **2013**, *135*, 9898−9906. (f) Rout, C. S.; Kim, B.-H.; Xu, X.; Yang, J.; Jeong, H. Y.; Odkhuu, D.; Park, N.; Cho, J.; Shin, H. S. *J. Am. Chem. Soc.* **2013**, *135*, 8720−8725. (g) Fei, H.; Li, H.; Li, Z.; Feng, W.; Liu, X.; Wei, M. *Dalton Trans.* **2014**, *43*, 16522−16527.

(10) (a) Bonadies, J. A.; Butler, W. M.; Pecoraro, V. L.; Carrano, C. J. *Inorg. Chem.* **1987**, *26*, 1218−1222. (b) Bonadies, J. A.; Pecoraro, V. L.; Carrano, C. J. *J. Chem. Soc., Chem. Commun.* **1986**, 1218−1219. (c) Tsuchida, E.; Oyaizu, K. *Coord. Chem. Rev.* **2003**, *237*, 213. (d) Oyaizu, K.; Tsuchida, E. *J. Am. Chem. Soc.* **2003**, *125*, 5630. (e) Oyaizu, K.; Tsuchida, E. *J. Am. Chem. Soc.* **1998**, *120*, 237. (f) Tsuchida, E.; Yamamoto, K.; Oyaizu, K.; Iwasaki, N.; Anson, F. C. *Inorg. Chem.* **1994**, *33*, 1056. (g) Oyaizu, K.; Dewi, E. L.; Tsuchida, E. *J. Electroanal. Chem.* **2001**, *498*, 136. (h) Galloni, P.; Coletti, A.; Floris, B.; Conte, V. *Inorg. Chim. Acta* **2014**, *420*, 144−148.

(11) Oyaizu, K.; Hayo, N.; Sasada, Y.; Kato, F.; Nishide, H. *Dalton Trans.* **2013**, *42*, 16090−16095.

(12) Hagfeldt, A.; Boschloo, G.; Sun, L.; Kloo, L.; Pettersson, H. *Chem. Rev.* **2010**, *110*, 6595−6663.

(13) Grätzel, M. *J. Photochem. Photobiol., C* **2003**, *4*, 145−153.

(14) Zhang, Z.; Chen, P.; Murakami, T. N.; Zakeeruddin, S. M.; Grätzel, M. *Adv. Funct. Mater.* **2008**, *18*, 341−346.

(15) Snaith, H. J.; Zakeeruddin, S. M.; Wang, Q.; Péchy, P.; Grätzel, M. *Nano Lett.* **2006**, *6*, 2000−2003.

(16) Cameron, P. J.; Peter, L. M.; Zakeeruddin, S. M.; Grätzel, M. *Coord. Chem. Rev.* **2004**, *248*, 1447−1453.

(17) Yanagida, S.; Yu, Y.; Manseki, K. *Acc. Chem. Res.* **2009**, *42*, 1827−1838.

(18) Boschloo, G.; Hagfeldt, A. *Acc. Chem. Res.* **2009**, *42*, 1819−1826.

(19) Gregg, B. A.; Pichot, F.; Ferrere, S.; Fields, C. L. *J. Phys. Chem. B* **2001**, *105*, 1422−1429.

(20) Yum, J.-H.; Baranoff, E.; Kessler, F.; Moehl, T.; Ahmad, S.; Bessho, T.; Marchioro, A.; Ghadiri, E.; Moser, J.-E.; Yi, C.; Nazeeruddin, M. K.; Grätzel, M. *Nat. Commun.* **2012**, *3*, 631.

(21) Neuthe, K.; Popeney, C. S.; Bialecka, K.; Hinsch, A.; Sokolowski, A.; Veurmann, W.; Haag, R. *Polyhedron* **2014**, *81*, 583−587.

(22) Wang, M.; Chamberland, N.; Breau, L.; Moser, J.-E.; Humphry-Baker, R.; Marsan, B.; Zakeerudin, M.; Grätzel, M. *Nat. Chem.* **2010**, *2*, 385−389.

(23) Fan, J.; Hao, Y.; Cabot, A.; Johansson, E. M. J.; Boschloo, G.; Hagfeldt, A. *ACS Appl. Mater. Interfaces* **2013**, *5*, 1902−1906.

(24) Nusbaumer, H.; Moser, J.-E.; Zakeeruddin, S. M.; Nazeeruddin, M. K.; Grätzel, M. *J. Phys. Chem. B* **2001**, *105*, 10461−10464.

(25) Xie, Y.; Hamann, T. W. *J. Phys. Chem. Lett.* **2013**, *2*, 328−332.

(26) Xiang, W.; Huang, F.; Cheng, Y. B.; Bach, C.; Spiccia, L. *Energy Environ. Sci.* **2013**, *6*, 121−127.

(27) Mathew, S.; Yella, A.; Gao, P.; Humphry-Baker, R.; Curchod, B. F. E.; Ashari-Astani, N.; Tavernelli, I.; Rothlisberger, U.; Nazeeruddin, M. K.; Grätzel, M. *Nat. Chem.* **2014**, *6*, 242−247.

(28) Vlasiou, M.; Drouza, C.; Kabanos, T. A.; Keramidas, A. D. *J. Inorg. Biochem.* **2015**, 00.

(29) Bard, A. J.; Stratmann, M. Inorganic Electrochemistry. In *Encyclopedia of Electrochemistry;* Bard, A. J.; Stratmann, M., Eds.; Wiley-VCH: Weinheim, Germany, 2006; Vol. *7*, pp 79−106.

(30) Gregg, B. A.; Pichot, F.; Ferrere, S.; Fields, S. C. L. *J. Phys. Chem. B* **2001**, *105*, 1422−1429.

(31) Li, T. C.; Spokoyny, A. M.; She, C.; Farha, O. K.; Mirkin, C. A.; Marks, T. J.; Hupp, J. T. *J. Am. Chem. Soc.* **2010**, *132*, 4580−4582.

(32) Rowe, R. A.; Jones, M. M. *Inorg. Synth.* **1957**, *5*, 113.

(33) Keramidas, A. D.; Papaioannou, A. B.; Vlahos, A.; Kabanos, T. A.; Bonas, G.; Makriyannis, A.; Raptopoulou, C. P.; Terzis, A. *Inorg. Chem.* **1996**, *35*, 357−367.

(34) The filtrate was cooled first to room temperature, then to 4 °C, and finally was left at −28 °C overnight.

(35) Stoll, S.; Schweiger, A. *J. Magn. Reson.* **2006**, *178*, 42−45.

(36) Stathatos, E.; Lianos, P.; Tsakiroglou, C. *Microporous Mesoporous Mater.* **2004**, *75*, 255−260.

(37) Makris, T.; Dracopoulos, V.; Stergiopoulos, T.; Lianos, P. *Electrochim. Acta* **2011**, *56*, 2004−2008.

(38) Yella, A.; Lee, H.-W.; Tsao, H. N.; Yi, C.; Chandiran, A. K.; Nazeeruddin, M. K.; Diau, E. W-G.; Yeh, C.-Y.; Zakeeruddin, S. M.; Grätzel, M. *Science* **2011**, *334*, 629−634.

(39) Bard, A. J.; Faulkner, L. R. *Electrochemical Methods, Fundamentals and Applications;* 2nd ed.; John Wiley & Sons: New York, 2001.

DOI: 10.1021/acs.inorgchem.5b00159
Inorg. Chem. XXXX, XXX, XXX−XXX

(40) Frisch, M. J.; Trucks, G. W.; Schlegel, H. B.; Scuseria, G. E.; Robb,M. A.; Cheeseman, J. R.; Scalmani, G.; Barone, V.; Mennucci, B.; Petersson, G. A.; Nakatsuji, H.;Caricato, M.; Li, X.; Hratchian, H. P.; Izmaylov, A. F.; Bloino, J.; Zheng, G.; Sonnenberg, J. L.; Hada,M.; Ehara, M.; Toyota, K.; Fukuda, R.; Hasegawa, J.; Ishida, M.; Nakajima, T.; Honda, Y.; Kitao, O.;Nakai, H.; Vreven, T.; Montgomery, J. A., Jr.; Peralta, J. E.; Ogliaro, F.; Bearpark, M.; Heyd, J. J.;Brothers, E.; Kudin, K. N.; Staroverov, V. N.; Kobayashi, R.; Normand, J.; Raghavachari, K.; Rendell, A.; Burant, J. C.; Iyengar, S. S.; Tomasi, J.; Cossi, M.; Rega, N.; Millam, N. J.; Klene, M.; Knox, J. E.;Cross, J. B.; Bakken, V.; Adamo, C.; Jaramillo, J.; Gomperts, R.; Stratmann, R. E.; Yazyev, O.;Austin, A. J.; Cammi, R.; Pomelli, C.; Ochterski, J. W.; Martin, R. L.; Morokuma, K.; Zakrzewski, V. G.;Voth, G. A.; Salvador, P.; Dannenberg, J. J.; Dapprich, S.; Daniels, A. D.; Farkas, Ö.; Foresman, J. B.; Ortiz, J. V.; Cioslowski, J.; Fox, D. J. *Gaussian 09,* Revision D.01; Gaussian, Inc.: Wallingford, CT, 2010.

(41) (a) Ernzerhof, M.; Scuseria, G. E. J. *Chem. Phys.* **1999**, *110*, 5029. (b) Adamo, C.; Barone, V. *Chem. Phys. Lett.* **1997**, *274*, 242. (c) Adamo, C.; Barone, V. J. *Chem. Phys.* **1999**, *110*, 6160. (d) Adamo, C.; Scuseria, G. E.; Barone, V. J. *Chem. Phys.* **1999**, *111*, 2889. (e) Adamo, C.; Barone, V. *Theor. Chem. Acc.* **2000**, *105*, 169. (f) Veter, V.; Adamo, C.; Maldivi, P. *Chem. Phys. Lett.* **2000**, *325*, 99.

(42) Tomasi, J.; Mennucci, B.; Cammi, R. *Chem. Rev.* **2005**, *105*, 2999.

(43) Shklover, V.; Ovchinnikov, Yu. E.; Braginsky, L. S.; Zakeeruddin, S. M.; Gratzel, M. *Chem. Mater.* **1998**, *10*, 2533.

(44) [$V^{IV}O(acac)_2$] was purified by dissolving it in the minimum quantity of boiling dichloromethane, filtering the solution, reducing the volume of the filtrate to ∼1/4 under reduced pressure, and, by dropwise addition of diethyl ether to the stirred solution, precipitating a deep green solid, which was filtered off and washed with diethyl ether.

(45) (a) Chasteen, D. N. *Biological Magnetic Resonance;* Berliner, L. J., Reuben, J., Eds.; Plenum Press: New York, 1981; Vol. 3, p 53. (b) Smith, T. S., II; LoBrutto, R.; Pecoraro, V. L. *Coord. Chem. Rev.* **2002**, *228*, 1−18. 38 (c) Mukherjee, T.; Costa Pessoa, J.; Kumar, A.; Sarkar, A. R. *Inorg. Chem.* **2011**, *50*, 4349−4361. (d) Lodyga-Chruscinska, E.; Micera, G.; Garribba, E. *Inorg. Chem.* **2011**, *50*, 883−899. (e) Gorelsky, S.; Micera, G.; Garribba, E. *Chem.—Eur. J.* **2010**, *16*, 8167−8180. (f) Smith Ii, T. S.; Root, C. A.; Kampf, J. W.; Rasmussen, P. G.; Pecoraro, V. L. *J. Am. Chem. Soc.* **2000**, *122*, 767−775. (h) Correia, I.; Pessoa, J. C.; Duarte, M. T.; Henriques, R. T.; Piedade, M. F. M.; Veiros, L. F.; Jakusch, T.; Kiss, T.; Dörnyei, Á.; Castro, M. M. C. A.; Geraldes, C. F. G. C.; Avecilla, F. *Chem.—Eur. J.* **2004**, *10*, 2301−2317.

(46) (a) Chatterjee, P. B.; Abtab, S. M. T.; Bhattacharya, K.; Endo, A.; Shotton, E. J.; Teat, S. J.; Chaudhury, M. *Inorg. Chem.* **2008**, *47*, 8830−8838. (b) Chatterjee, P. B.; Bhattacharya, K.; Chaudhury, M. *Coord. Chem. Rev.* **2011**, *255*, 2150−2164. (c) Chatterjee, P. B.; Bhattacharya, S.; Audhya, A.; Choi, K. Y.; Endo, A.; Chaudhury, M. *Inorg. Chem.* **2008**, *47*, 4891−4902. (d) Yamamoto, K.; Oyaizu, K.; Tsuchida, E. *J. Am. Chem. Soc.* **1996**, *118*, 12665−12672.

(47) (a) Tolis, E. J.; Teberekidis, V. I.; Raptopoulou, C. P.; Terzis, A.; Sigalas, M. P.; Deligiannakis, Y.; Kabanos, T. A. *Chem.—Eur. J.* **2001**, *7*, 2698−2710. (b) Aznar, C. P.; Deligiannakis, Y.; Tolis, E. J.; Kabanos, T. A.; Brynda, M.; Britt, R. D. *J. Phys. Chem. A* **2004**, *108*, 4310−4321.

(48) (a) Kato, F.; Hayashi, N.; Murakami, T.; Okumura, C.; Oyaizu, K.; Nishide, H. *Chem. Lett.* **2010**, *39*, 464. (b) Murakami, T.; Kato, F.; Oyaizu, K.; Nishide, H. *J. Photopolym. Sci. Technol.* **2010**, *23*, 353. (c) Lee, J.; Lee, C.; Lee, Y.; Cho, K.; Choi, J.; Park, J.-K. *J. Solid State Electrochem.* **2011**, *16*, 657. (d) Gryn'ova, G.; Barakat, J. M.; Blinco, J. P.; Bottle, S. E.; Coote, M. L. *Chem.—Eur. J.* **2012**, *18*, 7582.

(49) (a) Lenhardt, J.; Baruah, B.; Crans, D. C.; Johnson, M. D. *Chem. Commun.* **2006**, 4641−4643. (b) Waidmann, C. R.; Zhou, X.; Tsai, E. A.; Kaminsky, W.; Hrovat, D. A.; Borden, W. T.; Mayer, J. M. *J. Am. Chem. Soc.* **2009**, *131*, 4729−4743.

(50) Zhang, Y. *Inorg. Chem.* **1982**, *21*, 3886.

(51) Rehder, D.; Weidemann, C.; Duch, A.; Priebsch, W. *Inorg. Chem.* **1988**, *27*, 584.

(52) Kashif, M. K.; Nippe, M.; Duffy, N. W.; Forsyth, C. M.; Chang, C. J.; Long, J. R.; Spiccia, L.; Bach, U. *Angew. Chem., Int. Ed.* **2013**, *52*, 5527−5531.

(53) Kashif, M. K.; Axelson, J. C.; Duffy, N. W.; Forsyth, C. M.; Chang, C. J.; Long, J. R.; Spiccia, L.; Bach, U. *J. Am. Chem. Soc.* **2012**, *134*, 16646−16653.

(54) Roy, L. E.; Jakubikova, E.; Guthrie, M. G.; Batista, E. R. *J. Phys. Chem. A* **2009**, *113*, 6745−6750.

(55) Zare, H. R.; Eslami, M.; Namazian, M.; Coote, M. L. *J. Phys.Chem. B* **2009**, *113*, 8080.

(56) Tuttle, T. R.; Malaxos, S.; Coe, J. V. *J. Phys. Chem. A* **2002**, *106*, 925.

(57) Hardin, B. E.; Snaith, H. J.; McGehee, M. D. *Nat. Photonics* **2012**, *6*, 162.

(58) Mishra, A.; Fischer, M. K. R.; Bäuerle, P. *Angew. Chem., Int. Ed.* **2009**, *48*, 2474.

(59) Mao Liangwab, M.; Chen, J. *Chem. Soc. Rev.* **2013**, *42*, 3453.

DOI: 10.1021/acs.inorgchem.5b00159
Inorg. Chem. XXXX, XXX, XXX−XXX